http://dx.doi.org/10.1595/205651316X691960 *Johnson Matthey Technol. Rev.*, 2016, **60**, (3), 196–203

JOHNSON MATTHEY
TECHNOLOGY REVIEW

www.technology.matthey.com

Thermally Induced Deactivation and the Corresponding Strategies for Improving Durability in Automotive Three-Way Catalysts

A review of latest developments and fundamentals

By Jun-Jun He and Cheng-Xiong Wang
State Key Laboratory of Advanced Technologies for Comprehensive Utilization of Platinum Metals, Kunming Institute of Precious Metals, Kunming 650106, China

Ting-Ting Zheng
State-Local Joint Engineering Laboratory of Precious Metal Catalytic Technology and Application, Kunming Sino-platinum Metals Catalysts Co Ltd, Kunming 650106, China

Yun-Kun Zhao*
State Key Laboratory of Advanced Technologies for Comprehensive Utilization of Platinum Metals, Kunming Institute of Precious Metals, Kunming 650106, China; and State-Local Joint Engineering Laboratory of Precious Metal Catalytic Technology and Application, Kunming Sino-platinum Metals Catalysts Co Ltd, Kunming 650106, China

***Email:** yk.zhao@spmcatalyst.com

Increasingly demanding exhaust emissions regulations require that automotive three-way catalysts (TWC) must exhibit excellent catalytic activity and durability. Thus, developing TWC based on an accurate understanding of deactivation mechanisms is critical. This work briefly reviews thermally induced deactivation mechanisms, which are the major contributor to deactivation, and provides an overview of the common strategies for improving durability and preventing deactivation. It highlights the interaction of metals with supports and the diffusion inhibition of atoms and crystallites in both washcoats and metal nanoparticles and concludes with some recommendations for future research directions towards ever more challenging catalyst manufacture to meet increasing durability requirements both now and in the future.

1. Introduction

Concerns about the environment mean that new, increasingly demanding emissions standards have been gradually introduced around the world to improve urban air quality. California has the most demanding emissions legislation in the world. Its super ultra low emission vehicle ($SULEV_2$) standard mandates durability over 120,000 miles and the zero emission vehicle (ZEV_2) limits require up to 150,000 miles durability (1, 2). The typical exhaust gas temperatures of gasoline engines (≤800–850°C) are higher than those of diesel engines, but with very low start-up temperatures (≤250°C) that severely hinder hydrocarbon emissions control (3). In stoichiometric engines, close-coupled catalysts are exposed to bed-temperatures reaching 1050°C, resulting in difficulties in terms of the durability.

Therefore, both the catalytic activity and stability of the TWC must be carefully designed to meet both the stringent emissions norms and durability requirements.

There are many factors, for instance phase changes, poison adsorption, coking, mechanical and thermal lash, that can seriously affect the catalyst's structural and textural properties, metal dispersion, oxygen storage capacity (OSC) and redox activity (4, 5). The key deactivation mechanisms of catalysts are basically three-fold: chemical, mechanical and thermal. Thermal deactivation remains a fundamental problem to be resolved in TWC deactivation (6).

Compared with the base metals, precious metals are more commonly employed in automotive catalysts because of their intrinsic reactivity, preferable poisoning resistance and higher thermal stability that are required for automotive applications (7). However, precious metals also have intrinsic defects, for example particle growth and coalescence will occur under the complex reaction environment, resulting in rapid reduction of catalytic activity. This review is especially focused on providing an overview of the deactivation mechanisms in rare earth-based TWC and the corresponding strategies for improving durability.

2. Oxide Washcoat Materials

Alumina is employed as the most common washcoat material in TWC owing to its excellent chemical and thermal stability. Ceria-based additives play a critical role in providing oxygen mobility and oxygen storage in TWC due to their recognised ability to undergo rapid reduction/oxidation cycles, according to Equation (i) (8):

$$4CeO_2 \rightleftharpoons 2Ce_2O_3 + O_2 \quad \text{(i)}$$

However, Al_2O_3 and CeO_2-based materials, as the main components of washcoats, are subjected to significant sintering as presented in **Figure 1**. Sintering is seen as one of the major deactivation mechanisms (4, 9). Washcoat sintering typically occurs at very high temperatures with coalescence and growth of particles as well as collapse and elimination of pores leading to a decrease of the specific surface area and encapsulation of active metal nanoparticles by washcoat, as well as a sharp loss of active surface area.

In the case of Al_2O_3, sintering is accompanied by thermally induced phase transformation. According to Arai and coworkers, γ-Al_2O_3 (100–200 m^2 g^{-1} surface area) undergoes consecutive and irreversible phase transformation at high temperatures (10). The

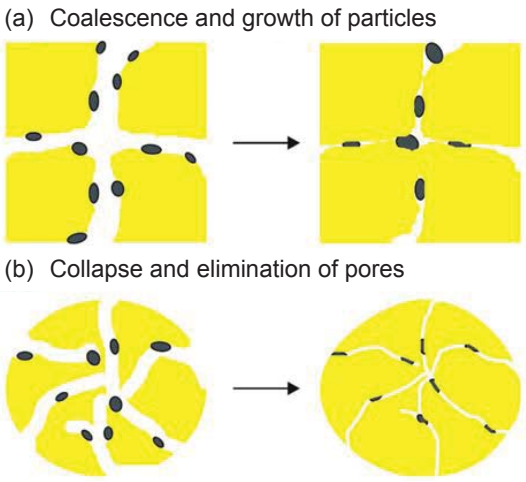

Fig. 1. Thermally induced changes take place in washcoat materials

porous γ-Al_2O_3 starts to turn gradually to δ-Al_2O_3 at an approximate temperature of 900°C, which successively changes to θ-Al_2O_3 at approximately 1000°C and finally to non-porous α-Al_2O_3 (only ~5 m^2 g^{-1} surface area) above 1200°C (7, 11), which results from the coalescence of particles and the elimination of pore structures.

Compared to other washcoat materials for TWC, Al_2O_3 has a higher specific surface area and better thermal and chemical stability that is particularly significant for metal dispersion. Hence, improving skeleton stability and suppressing phase transformation of γ-Al_2O_3 are necessary. These can be achieved through skeletal doping with specific dopants (i.e. lanthanum oxide (La_2O_3), zirconia (ZrO_2) and yttrium(III) oxide (Y_2O_3)). Inserting metal ions (especially La^{3+} with a large ionic radius) into the skeleton of transitional Al_2O_3 to prevent the diffusion of O^{2-} and Al^{3+} ions should be the most effective strategy for improving thermal stability. However, atomic scale insertion is still a technical challenge and remains an interesting research field.

CeO_2 readily crystallises and sinters with growth of particles and loss of surface area, leading to rapid reduction of the oxygen storage and release properties that are the most critical feature of TWC. Similarly, the formation of CeO_2-ZrO_2 solid solution achieved through introduction of Zr^{4+} ions into the CeO_2 skeleton not only stabilises the host lattice of crystalline CeO_2 at high temperatures, but also enhances the catalytic activities of water-gas shift reactions and hydrocarbon steam-reforming reactions in catalytic converters (12, 13).

CeO_2-ZrO_2 mixed oxides have a surface area below 2 m^2 g^{-1} and the particles undergo significant coalescence and growth. One study found a crystallite size of 19.6 nm after thermal treatment at 1000°C for 5 hours under static air (14). Although total oxygen storage capacity (OSC-cI) and the amount of O_2 adsorption/desorption per mol of CeO_2 (OSC-cII) showed no obvious changes, the oxygen release rate (OSC-r) suffered a sharp decrease as shown in **Table I**.

For the further improvement of stability of the CeO_2-ZrO_2 composite, ternary CeO_2-based composite materials were introduced. As Lee's group reported, La^{3+} and Sm^{3+} can effectively stabilise the cubic $Ce_{0.40}Zr_{0.60}O_2$ phase that plays a critical role in oxygen mobility and OSC, while other rare earth elements have the opposite effect (15). The ternary component content also affects the OSC stability according to Chen *et al.* (16): a high neodymium content will gradually convert the CeO_2-ZrO_2 cubic phase into a $Nd_{0.50}Zr_{0.50}O_{1.75}$ cubic phase which leads to a decline in the OSC.

Table I Properties of CeO_2-ZrO_2 Mixed Oxides

Properties	Fresh sample	Aged sample
OSC-cI, μmol g_{cat}^{-1}	317	225
OSC-cII, mol mol^{-1} CeO_2	0.102	0.073
OSC-r, μmol g_{cat}^{-1} s	13.1	0.3
Crystallite size, nm	8.4	19.6

Another strategy for improving the stability of CeO_2-ZrO_2 materials is the use of Al_2O_3 particles as diffusion barriers, introduced to form Al_2O_3-CeO_2-ZrO_2 hybrid oxides as shown in **Figure 2**. Compared to CeO_2-ZrO_2 mixed oxides, the Al_2O_3-CeO_2-ZrO_2 hybrid oxides still have a high surface area and OSC after durability ageing under the same conditions (14). There is however difficulty in controlling the metal-support interfaces which may have a negative effect on particular reactions occurring in the catalytic converter (17). The most negative influence for automotive exhaust catalysts is the formation of rhodium aluminate compounds at the Rh-Al_2O_3 interface (18).

As mentioned above, strategies that simultaneously take into account catalyst stability and control of the metal-support interface should be developed, to ensure high activity and sufficient durability, which are then able to meet upcoming emission standards. This is a promising research field but with some great technological challenges.

3. Active Precious Metals

Besides a sufficient washcoat surface area, two other key contributors to high catalytic activity are the surface area and dispersion of the precious metal nanoparticles. Over time in operation, the active precious metal nanoparticles will be subjected to crystallite growth due to sintering, resulting in reduced activity, even to the point of total deactivation.

Atomic and crystallite migration are two hypotheses for sintering of supported catalysts (19) as shown

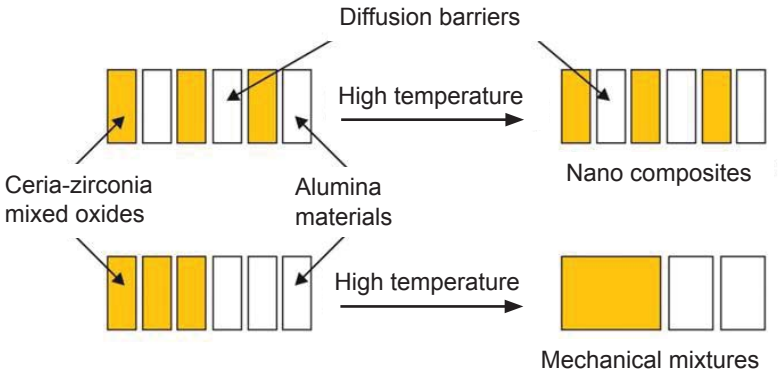

Fig. 2. Schematic illustration of Al_2O_3 particles as diffusion barriers in CeO_2-ZrO_2 mixed oxides to improve washcoat thermal stability

in **Figure 3**. In these cases, particle migration and coalescence (PMC) and Ostwald ripening (OR) are the two main sintering mechanisms according to Bowker (20). Both PMC and OR are dynamic processes which involve atomic exchange. The PMC sintering mechanism occurs when two or more particles touch or collide and then merge to form a larger particle. In contrast, the OR sintering mechanism occurs when material evaporates from the surface of a smaller particle with higher surface energy, and transfers onto the surface of a larger particle.

Sintering of active precious metal nanoparticles is closely related to reaction temperature and the size and composition of the nanoparticles (17). When quasi-liquid layers form on the crystal surface, migration of surface atoms and crystallites will occur at the Hüttig or Tamman temperatures of the bulk phase that are often used to semi-empirically describe the temperatures at which atomic migration and crystallite migration can occur. The ratio of the melting point ($T_{melting}$) of unique particles with radius, r, and heat of fusion, L, to that of the bulk phase (T_0) can be given by Equation (ii) (21):

$$\frac{T_{melting}}{T_0} = 1 - \frac{2}{\rho_s L r}\left\{\gamma_s - \gamma_l\left(\frac{\rho_s}{\rho_l}\right)^{2/3}\right\} \quad \text{(ii)}$$

where γ and ρ represent the surface free energy and density of the solid and liquid, respectively. **Table II** exhibits T_0, T_{Tamman} and $T_{Hüttig}$ of platinum, palladium, Rh and their compounds. Metallic Pt, Pd and Rh have higher Hüttig and Tamman temperatures than the corresponding compounds, demonstrating that higher valency metals may have poorer thermal stability. Equation (ii) highlights that the melting point of unique particles depends on their composition, size and also surface free energy.

The experimental observations show that temperature is a dominant factor for sintering (22). The sintering behaviours of active precious metals can also be affected by any other conditions that lead to changes in the surface energy of the particles, such as reaction atmosphere (23), shape and composition of metal nanoparticles (24), metal dispersion (25), the loading of the metal on supports (26) and the interactions between the supports and metals (27).

Table II T_0, T_{Tamman} and $T_{Hüttig}$ Values of Pt, Pd, Rh and their Compounds

Metals	T_0, K	T_{Tamman}, K	$T_{Hüttig}$, K
Pt	2028	1014	608
PtO	823	412	247
PtO_2	723	362	217
$PtCl_2$	854	427	256
$PtCl_4$	643	322	193
Pd	1828	914	548
PdO	1023	512	307
Rh	2258	1129	677
Rh_2O_3	1373	687	412

Higher durability requires a lower sintering rate to maintain enough metal surface for long-term use and this is often accomplished through stabilising the active metal nanoparticles. **Figure 4** shows the three typical strategies for precious metal sintering suppression (28–30): (a) support anchoring for metal nanoparticles, (b) alloying of active metals and (c) inhibition of atomic and crystallite migration *via* support encapsulation technology, for instance the construction of core-shell nanostructures and atomic layer deposition. In TWC,

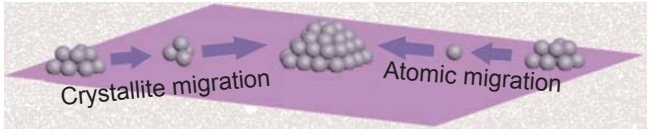

Fig. 3. Two conceptual models for sintering of active precious metal particles

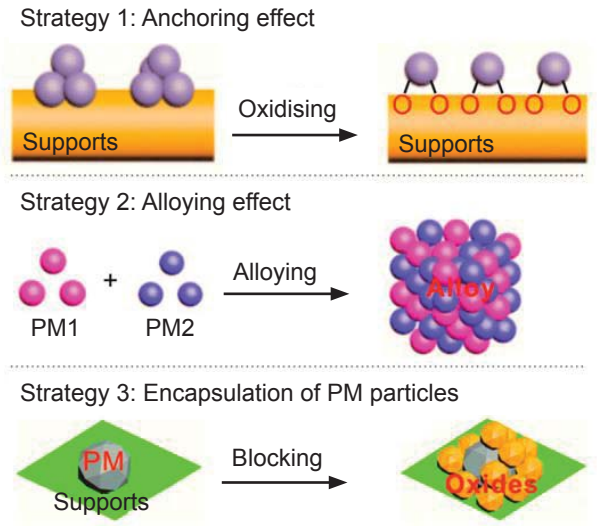

Fig. 4. Three typical strategies for precious metal sintering suppression in TWC

precious metal sintering is difficult to suppress by support anchoring due to the fluctuations of exhaust gas compositions and temperatures under operating conditions. In addition, support anchoring effects only occur at given temperature windows (31). Alloying by the introduction of a second metal with a higher melting point is a simpler and more controllable way to control metal sintering and improve thermal durability. Hence, additional composition and content optimisation of bimetallic catalysts for better self-stabilisation effect may be of great importance. However, according to our years of experience, alloying is both difficult to control and to avoid the negative metal-support interactions for industrial applications remains a challenge.

For the third strategy, support encapsulation technology can form additional metal-support interfaces, but both the stability of shells in core-shell nanostructure catalysts and the cost of atomic layer deposition technology still require further technical breakthroughs.

4. Redispersion and Regeneration

The metal dispersion and sintering rates of supported metal catalysts strongly depend on ageing atmosphere, as shown in **Table III** (32), indicating that the atmosphere found in exhaust gases can accelerate the deactivation rate over that seen in inert atmosphere. It is noted that redispersion is the opposite process to sintering. The reactant-induced disintegration of the active phase is of great importance in redispersion of active precious metals for long-term use. The disintegration strongly depends on the formation rate of adatom complexes such as PtO_x, $Pd(CO)_x$ and $Rh(NO)_x$. These adatoms will form when metal-metal or metal-support interactions are replaced by metal-reactant bonds (33). Newton

Table III Effect of Ageing Atmosphere on the Metal Dispersion and Sintering Behaviour

Ageing atmosphere	Pt	Pd	Rh
N_2, 1100°C	21 nm	97 nm	14 nm
Simulated exhaust gas, 1100°C	78 nm	68 nm	88 nm
Air, 1100°C	97 nm	not determined	not determined

et al. found that Pd nanoparticle redispersion occurs during CO/NO cycling, which points to the formation of $Pd(CO)_x$ and $Pd(NO)_x$ adatom complexes (34).

Sintering and redispersion occur under reducing and oxidising atmospheres, respectively (35). Similar phenomena can be observed in Rh-based catalysts as well as Pt-based catalysts (36, 37). Thus, redispersion of the active phase in TWC might be interpreted as shown in **Figure 5**. The redispersion of precious metal particles in TWC can be achieved in two ways: disintegration or oxidation. The changes of chemical states that affect oxidation reactions largely depend on air-to-fuel ratio fluctuations and operating temperatures (38).

Grunwaldt's group found that regeneration of deactivated bimetallic catalysts could be achieved by hydrogen reduction due to the formation of alloyed particles leading to enhanced oxidation activity under lean combustion conditions (39). This regeneration mechanism entirely differs from reduction-induced sintering because oxidation improves the precious metal dispersion for monometallic catalysts while the opposite is seen during the reduction process.

As reported by Birgersson's group, regeneration of TWC can also be achieved through a thermal treatment under an atmosphere containing chlorine

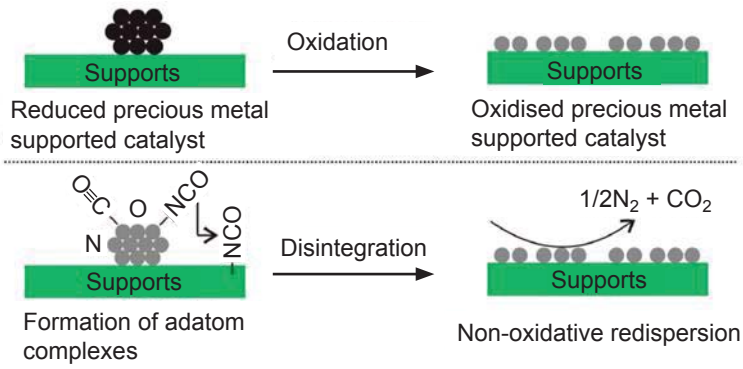

Fig. 5. A schematic representation of redispersion for active precious metals

(40). However, it should be noted that oxy-chlorination may cause a narrow temperature window for oxidation of metallic species and the loss of precious metals due to the formation of volatile MO_xCl_y compounds. In the case of Pt, $Pt(OH)_xCl_y$ and α-PtO_2 will transform into PtO_xCl_y above 500°C, resulting in Pt loss, as reported by Lieske *et al.* (41). Christou and coworkers reported a new 'oxalic acid' regeneration methodology for aged commercial TWC without any negative effects, which may be a promising method for further investigation to improve durability (42). In our experience, however, artificial regeneration of TWC is difficult to achieve for industrial applications. Thus, these regeneration methods are considered undesirable for improvement of durability of TWC and more attention should be given to other strategies.

The composition of gasoline engine tail-pipe emissions fluctuates quickly and dramatically between oxidation and reduction environments during operation. This makes 'on-board' redispersion and regeneration of TWC highly unsuitable and hardly controllable. CeO_2, used as the most common additive in TWC, provides oxygen mobility capability from the surface of CeO_2 to precious metal particles and promotes the dispersion of active metals (43). Nagai *et al.* reported that the stability of oxidation states depends on the precious metal oxide-support interaction (44). In our opinion, improving the oxygen activation properties of CeO_2 and optimising the interaction between precious metals and CeO_2 should be investigated to enhance the redispersion and regeneration capability of the active phase.

5. Conclusions

Thermally induced deactivation mechanisms are attributed to metal surface loss and the sharp decline of washcoat specific surface area as well as the collapse of pore structures caused by sintering. Redispersion and regeneration phenomena of TWC are only experimental observations and there is still a long development path towards industrial application due to real-world challenges and exhaust gas composition that can actually accelerate deactivation. To improve the durability of TWC, further attention should be given to understanding the metal-support interactions and the diffusion inhibition of atoms and crystallites in order to reduce the sintering rate of the precious metal and stabilise the structure of washcoats. Inserting specific ions into the skeleton of Al_2O_3 and CeO_2-ZrO_2 mixed oxides is an effective method for improving structure stability, but atomic scale insertion still presents a challenge in manufacture. In our opinion, the use of alloying effects to stabilise precious metal nanoparticles is very helpful for the improvement of thermal durability. Nevertheless, further optimising the composition and content of the alloys and reducing undesirable metal-support interactions still pose great challenges in TWC application and manufacture.

Acknowledgements

The authors are grateful for support by the National Natural Science Foundation of China (21463015) and the Provincial Natural Science Foundation of Yunnan, China (2014FA045).

References

1. M. V. Twigg, *Catal. Today*, 2011, **163**, (1), 33
2. M. V. Twigg, *Platinum Metals Rev.*, 2011, **55**, (1), 43
3. J. Kašpar, P. Fornasiero and N. Hickey, *Catal. Today*, 2003, **77**, (4), 419
4. A. Fathali, L. Olsson, F. Ekström, M. Laurell and B. Andersson, *Top. Catal.*, 2013, **56**, (1), 323
5. D. M. Fernandes, C. F. Scofield, A. A. Neto, M. J. B. Cardoso and F. M. Z. Zotin, *Chem. Eng. J.*, 2010, **160**, (1), 85
6. S. Matsumoto, *Catal Today*, 2004, **90**, (3–4), 183
7. U. Lassi, 'Deactivation Correlations of Pd/Rh Three-way Catalysts Designed for Euro IV Emission Limits: Effect of Ageing Atmosphere, Temperature and Time', PhD Thesis, Department of Process and Environmental Engineering, University of Oulu, Finland, 2003
8. G. Balducci, P. Fornasiero, R. D. Monte, J. Kaspar, S. Meriani and M. Graziani, *Catal. Lett.*, 1995, **33**, (1), 193
9. D. M. Fernandes, C. F. Scofield, A. A. Neto, M. J. B. Cardoso and F. M. Z. Zotin, *Process Saf. Environ.*, 2009, **87**, (5), 315
10. F. M. Z. Zotin, O. da Fonseca Martins Gomes, C. H. de Oliveira, A. A. Neto and M. J. B. Cardoso, *Catal Today*, 2005, **107–108**, 157
11. P. A. Badkar and J. E. Bailey, *J. Mater. Sci.*, 1976, **11**, (10), 1794
12. T. Kolli, K. Rahkamaa-Tolonen, U. Lassi, A. Savimäki and R. L. Keiski, *Catal Today*, 2005, **100**, (3–4), 297
13. L. Jia, M. Shen and J. Wang, *Surf. Coat. Tech.*, 2007, **201**, (16–17), 7159

14. A. Morikawa, T. Suzuki, T. Kanazawa, K. Kikuta, A. Suda and H. Shinjo, *Appl. Catal. B: Eviron.*, 2008, **78**, (3–4), 210
15. D. H. Prasad, S. Y. Park, H.-I. Ji, H.-R. Kim, J.-W. Son, B.-K. Kim, H.-W. Lee and J.-H. Lee, *J. Phys. Chem. C*, 2012, **116**, (5), 3467
16. J. Guo, Z. Shi, D. Wu, H. Yin, M. Gong and Y. Chen, *J. Alloy Compd.*, 2015, **621**, 104
17. M. Shen, M. Yang, J. Wang, J. Wen, M. Zhao and W. Wang, *J. Phys. Chem. C*, 2009, **113**, (8), 3212
18. V. Marchionni, M. A. Newton, A. Kambolis, S. K. Matam, A. Weidenkaff and D. Ferri, *Catal. Today*, 2014, **229**, 80
19. C. H. Bartholomew, *Appl. Catal. A: Gen.*, 2001, **212**, (1–2), 17
20. M. Bowker, *Nature Mater.*, 2002, **1**, (4), 205
21. Ph. Buffat and J.-P. Borel, *Phys. Rev. A*, 1976, **13**, (6), 2287
22. P. Forzatti and L. Lietti, *Catal Today*, 1999, **52**, (2–3), 165
23. J. A. Moulijn, A. E. van Diepen and F. Kapteijn, *Appl. Catal. A: Gen.*, 2001, **212**, (1–2), 3
24. A. Cao and G. Veser, *Nature Mater.*, 2010, **9**, (1), 75
25. X. Yan, X. Wang, Y. Tang, G. Ma, S. Zou, R. Li, X. Peng, S. Dai and J. Fan, *Chem. Mater.*, 2013, **25**, (9), 1556
26. W. Zou and R. D. Gonzalez, *Appl. Catal. A: Gen.*, 1993, **102**, (2), 181
27. H. Shinjoh, M. Hatanaka, Y. Nagai, T. Tanabe, N. Takahashi, T. Yoshida and Y. Miyake, *Top. Catal.*, 2009, **52**, (13–20), 1967
28. M. Cargnello, J. J. D. Jaén, J. C. Hernández Garrido, K. Bakhmutsky, T. Montini, J. J. Calvino Gámez, R. J. Gorte and P. Fornasiero, *Science*, 2012, **337**, (6095), 713
29. A. A. Vedyagin, M. S. Gavrilov, A. M. Volodin, V. O. Stoyanovskii, E. M. Slavinskaya, I. V. Mishakov and Y. V. Shubin, *Top. Catal.*, 2013, **56**, (11), 1008
30. J. Lu, B. Fu, M. C. Kung, G. Xiao, J. W. Elam, H. H. Kung and P. C. Stair, *Science*, 2012, **335**, (6073), 1205
31. S. Hinokuma, H. Fujii, Y. Katsuhara, K. Ikeue and M. Machida, *Catal. Sci. Technol.*, 2014, **4**, (9), 2990
32. H. Shinjoh, H. Muraki and Y. Fujitani, *Stud. Surf. Sci. Catal.*, 1991, **71**, 617
33. B. R. Goldsmith, E. D. Sanderson, R. Ouyang and W.-X. Li, *J. Phys. Chem. C*, 2014, **118**, (18), 9588
34. M. A. Newton, C. Belver-Coldeira, A. Martínez-Arias and M. Fernández-García, *Nature Mater.*, 2007, **6**, (7), 528
35. R. J. Farrauto, M. C. Hobson, T. Kennelly and E. M. Waterman, *Appl. Catal. A: Gen.*, 1992, **81**, (2), 227
36. A. J. Dent, J. Evans, S. G. Fiddy, B. Jyoti, M. A. Newton and M. Tromp, *Angew. Chem. Int. Ed.*, 2007, **46**, (28), 5356
37. S. Bernal, G. Blanco, J. J. Calvino, J. M. Gatica, J. A. Pérez Omil and J. M. Pintado, *Top. Catal.*, 2004, **28**, (1), 31
38. J. Kašpar, P. Fornasiero and N. Hickey, *Catal. Today*, 2003, **77**, (4), 419
39. A. T. Gremminger, H. W. P. de Carvalho, R. Popescu, J.-D. Grunwaldt and O. Deutschmann, *Catal. Today*, 2015, **258**, (2), 470
40. H. Birgersson, M. Boutonnet, S. Järås and L. Eriksson, *Top. Catal.*, 2004, **30**, (1), 433
41. H. Lieske, G. Lietz, H. Spindler and J. Völter, *J. Catal.*, 1983, **81**, (1), 8
42. S. Y. Christou, J. Gåsste, H. L. Karlsson, J. L. G. Fierro and A. M. Efstathiou, *Top. Catal.*, 2009, **52**, (13–20), 2029
43. M. Hatanaka, N. Takahashi, N. Takahashi, T. Tanabe, Y. Nagai, A. Suda and H. Shinjoh, *J. Catal.*, 2009, **266**, (2), 182
44. Y. Nagai, K. Dohmae, Y. Ikeda, N. Takagi, T. Tanabe, N. Hara, G. Guilera, S. Pascarelli, M. A. Newton, O. Kuno, H. Jiang, H. Shinjoh and S. Matsumoto, *Angew. Chem. Int. Ed.*, 2008, **47**, (48), 9303

The Authors

Jun-Jun He graduated from Tianjin University, China, in 2011, with a PhD in Chemical Engineering and Technology and subsequently worked as a Research and Design Engineer at Kunming Institute of Precious Metals (IPM), China. His main research field is new washcoat recipe design and applications. He is also Head of the gasoline aftertreatment team at IPM.

Cheng-Xiong Wang obtained a Bachelor of Engineering degree in Chemical Engineering from Taiyuan University of Technology, China, in 2013. He is currently pursuing his Master's degree in Catalysis Science at IPM.

Ting-Ting Zheng has a Bachelor's degree in Chemical Engineering from Northwestern University, China, and a Master's degree in Catalysis Science from IPM. She works at State-Local Joint Engineering Laboratory of Precious Metal Catalytic Technology and Application and is devoted to the research and development of TWC in emissions control.

Dr Yun-Kun Zhao received his PhD from Lanzhou University, China, and had a postdoctoral career at Peking University, China. As a Senior Professor at IPM, he has specialised in platinum group metals assaying methods and catalytic materials development. Since 2002, he is Technical Director at Kunming Sino-Platinum Metals Catalysts Co Ltd. His main responsibility is to develop catalysts for exhaust emissions control.